Diffraction Measurements of Load Transfer in Interpenetrating-Phase Al_2O_3/Al Composites

M.L. Young,[1] J.D. Almer,[2] U. Lienert,[2] D.R. Haeffner,[2] R. Rao,[3] J.A. Lewis,[3] D.C. Dunand[1]
[1]Department of Materials Science and Engineering, Northwestern University, Evanston, IL, U.S.A.
[2]Advanced Photon Source (APS), Argonne National Laboratory, Argonne, IL, U.S.A.
[3]Department of Materials Science and Engineering, University of Illinois at Champaign-Urbana, Urbana, IL, U.S.A.

Introduction

Interpenetrating-phase composites (IPCs) are characterized by two co-continuous and percolating phases. Ceramic-metal IPCs typically exhibit much greater toughness than pure ceramics (e.g., cermets such as WC-Co with high metals content). Methods for creating ceramic-metal IPCs with a very regular architecture and tailored properties are described in more detail in Ref. 1. Complex 3-D ceramic architectures were created by robocasting in a layerwise manner [2-4].

In this report, we examine an interpenetrating Al_2O_3-Al composite produced by liquid metal infiltration of 3-D periodic Al_2O_3 preforms of varying lattice geometry. The IPCs were subjected to uniaxial compressive stresses while internal strains were measured by synchrotron x-ray diffraction. The extent of load transfer between the two phases was measured for each preform geometry.

Methods and Materials

Composite Processing

Al_2O_3 towers, consisting of 30 alternating 0/90 layers of parallel rods, were produced by robotic deposition by using a gel-based ink described in more detail in Ref. 5. The Al_2O_3 towers were created with simple-cubic symmetry or fcc symmetry as described in Ref. 1. After assembly, the 30-layer tower structures were dried in air for 24 hours and then sintered in air at 1600°C for 2.5 hours. The final rod diameter was approximately 250 mm in the densified structures. Subsequently, the sintered Al_2O_3 towers were gas-pressurized and liquid-metal-infiltrated with 99.99% pure aluminum.

Synchrotron X-ray Diffraction

X-ray measurements were made at two APS beamline stations: XOR 1-ID-C and BESSRC 11-ID-B. *In situ* mechanical testing was performed by using a small, custom-built, screw-driven loading system for uniaxial testing. The general setup for these experiments is described in detail in Ref. 6 and is shown schematically in Fig. 1.

Two samples, each one with fcc symmetry and simple-cubic symmetry for the alumina phase, were subjected to uniaxial compressive loading with about 30-MPa load increments. At each load level, diffraction measurements were performed with a monochromatic 81-keV (λ = 0.015 nm) x-ray beam for 20 to 60 seconds. The x-ray beam generally had a square cross section of 150 × 150 μm^2. Complete Debye-Scherrer diffraction cones from the crystalline phases present in the diffraction volumes were recorded by using an image plate (Mar345). Additional calibration diffraction cones were produced from a paste composed of vacuum grease and pure ceria powder, which was smoothly applied to one surface of each sample. The image plate had a 345-mm diameter and was operated in full mode, providing a 100-mm pixel size with a 16-bit dynamic range. The sample-to-camera distance was 1.220 m. The samples were positioned with their vertical faces perpendicular/parallel to the beam. The beam was positioned in the center of the face such that the transmitted intensity was maximal, corresponding to a region with the highest local alumina content. Since the beam width (150 μm) is smaller than the Al_2O_3 strut width (about 250 μm), the beam path was within a horizontal rod.

A typical diffraction pattern for an interpenetrating-phase Al/Al_2O_3 composite is shown in Fig. 2. Determination of lattice strains from the diffracted rings recorded by the camera consisted of the following steps. First a Fit2D macro was used to determine the beam center and the tilt. Then the image was caked, integrated, and outputted to a 16-bit tif file. Matlab programs were then used to do pseudo-Voigt peak fits on selected ceria and alumina peaks and to determine lattice strains from peak positions as a function of azimuth by using equations from Ref. 7.

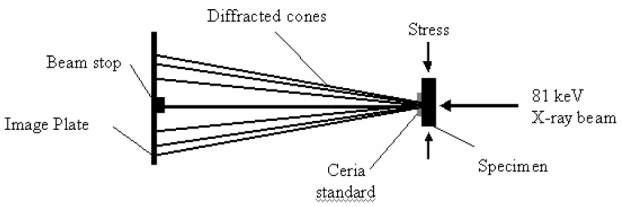

FIG. 1. Schematic of experimental setup.

Results

As seen in Fig. 2, the rings for the Al phase were spotty because of the large grain size of aluminum (due to the casting method) compared to the irradiated volume. Thus, no strain could be measured for the matrix. The Al_2O_3 phase exhibits complete rings, as expected from the fine grain size of the alumina processed as described above.

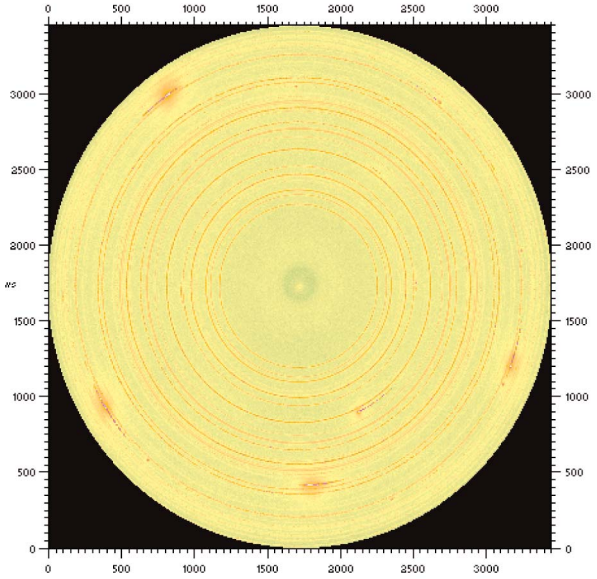

FIG. 2. Typical x-ray diffraction pattern for interpenetrating-phase Al/Al_2O_3 composites. Complete rings belong to the alumina and ceria phases, while partial rings belong to the Al phase.

Face-centered-cubic Symmetry Composite

The sample with fcc symmetry had a density of 3.42 g/cm^3, corresponding to an Al volume fraction of 43.6%. This sample was tested to failure, which occurred at 240 MPa. This value is much lower than that measured previously on similar simple-cubic composites (700 MPa [15]), which is inherently stronger, because the vertical columns are straight (unlike those for the face-centered towers). Another possibility is that damage occurred during machining, which exposed the alumina phase.

The elastic lattice strain for (300) planes versus the applied stress for the fcc symmetry composite is shown in Fig. 3. Similar plots were obtained for other (hkl) planes and are not presented here. The apparent elastic modulus of the alumina phase (E_{app} = 316 GPa, defined as the applied stress divided by average lattice strain e_{22} in the same direction as the applied stress) was lower than the elastic modulus of pure Al_2O_3 (E = 410 GPa). This effect was due to load transfer from the aluminum to the alumina phase and indicates that the stress carried

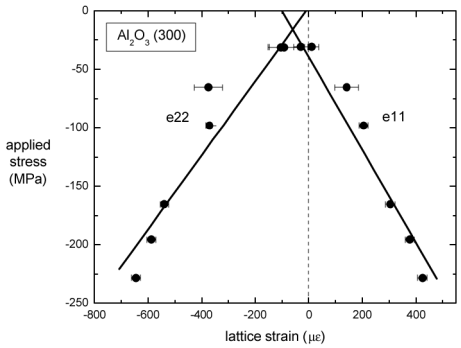

FIG. 3. Applied stress versus lattice strain for Al/Al_2O_3 composites with fcc symmetry, by using (300) reflection, upon increasing the stress (mechanical loading).

by the alumina phase is higher than the applied stress, as observed in many other metal-ceramic systems (e.g., see Refs. 8 and 9). Modeling is complicated by the fact that the volume measured consists of columns (mostly under uniaxial compressive stress) and struts, whose stress states are unknown and dictated by load transfer from both the adjacent Al phase and the adjacent alumina columns. However, it is apparent that the average elastic strain e_{22} is negative (i.e., compressive in nature). The average elastic strains e_{11} perpendicular to the direction of the applied load are positive, and the apparent modulus is E_{app} = 398 GPa, very close to the value of the elastic modulus of pure Al_2O_3. Thus, the average state of stress of the alumina phase seems to be close to uniaxial compressive (with strains $e_{22} = -\upsilon\, e_{11}$, where υ is the Poisson's ratio). Finally, it is apparent that residual strains are present under zero applied stress, as expected from the mismatch in thermal expansion between the two phases.

Simple-cubic Symmetry Composite

The simple-cubic symmetry sample exhibited a density of 3.53 g/cm^3, corresponding to an Al volume fraction of 34.8%. This sample was cycle tested from 0 to 225 to 0 MPa without failure. Similar to the fcc symmetry sample, plots of the applied stress versus lattice strain were created for several Al_2O_3 (hkl) planes. Such plots for Al_2O_3 (300) planes, which are representative of typical (hkl) planes, are presented in Fig. 4.

Upon uniaxial loading of the composite, the average lattice strains of the alumina phase increase linearly with the applied stress (top of Fig. 4), as they did for the fcc symmetry sample (Fig. 3). The apparent moduli (E_{app} = 202 and 291 GPa in the e_{22} and e_{11} directions, respectively) are lower than they were for the sample with fcc symmetry, indicative of an increase in load transfer from the metal to the ceramic phase. Upon subsequent unloading, the apparent elastic moduli are

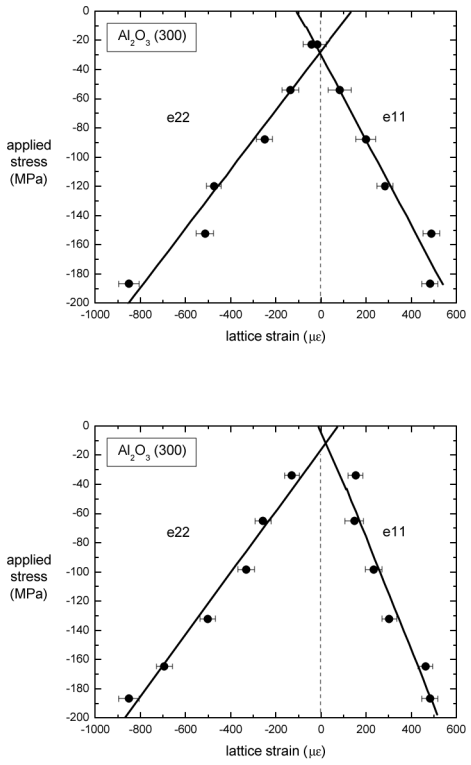

FIG. 4. Applied stress versus lattice strain for Al/Al_2O_3 composites with simple-cubic symmetry by using (300) reflection, upon increasing the stress (mechanical loading) (top) and upon decreasing the stress (mechanical unloading) (bottom).

E_{app} = 211 and 384 GPa in the e_{22} and e_{11} directions, respectively (bottom of Fig. 4). Superposing the top and bottom of Fig. 4 shows that the data on loading and unloading are, within experimental error, the same. This indicates that no large-scale damage occurred (e.g., by fracture of the alumina phase or delamination of the interface), since such damage would alter the extent of load transfer.

A detailed finite-element analysis will be needed to clarify the distribution of stresses and strains in the measured alumina volume, both under zero and nonzero applied loads. The model will take into account matrix plasticity, which is expected at the lowest applied stresses but constrained by the presence of the interconnected elastic alumina phase.

Discussion

Interpenetrating Al_2O_3-Al composites were produced by liquid metal infiltration of a 3-D periodic Al_2O_3 preform with spanning elements that were fabricated by robotic deposition. Two preforms were used, with simple-cubic and fcc symmetry, respectively. These interpenetrating composites were compressed uniaxially while interrogated by high-energy x-ray diffraction. The results indicate that load transfer is occurring between the two phases, more so for the composite with the simple-cubic alumina phase. For that composite, no change in load transfer was observed upon unloading from 200 MPa, indicating that damage was absent.

Acknowledgments

R. Rao and J.A. Lewis acknowledge funding provided by National Science Foundation Grant No. DMI-00-99360. The robocasting apparatus used in this work was designed and built by J. Cesarano, and customized software for 3-D fabrication was developed by J.E. Smay. Use of the APS was supported by the U.S. Department of Energy, Office of Science, Office of Basic Energy Sciences, under Contract No. W-31-109-ENG-38. D. Shu (APS) built the compression rig.

References

[1] M.L. Young, J.D. Almer, U. Lienert, D.R. Haeffner, R. Rao, J.A. Lewis, D.C. Dunand, paper presented at the Materials Science & Technology Conference (Chicago, IL, 9-12 November 2003).
[2] J. Cesarano and P. Calvert, U.S. Patent No. 6,027,326 (2000).
[3] J.E Smay, G.M. Gratson, R.F. Shepherd, J. Cesarano, and J.A. Lewis, Adv. Mater. **14**, 1279 (2002).
[4] J.E. Smay, J. Cesarano, and J.A. Lewis, Langmuir **18**, 5429 (2002).
[5] C. San Marchi, M. Kouzeli, R. Rao, J.A. Lewis, and D.C. Dunand, Scripta Mater. (in print, 2003).
[6] A. Wanner and D.C. Dunand, Metall. Mater. Trans. **31**, 2949 (2000).
[7] B.B.He and K.L. Smith, paper presented at the Society for Experimental Mechanics (SEM) Spring Conference on Experimental and Applied Mechanics and Experimental/Numerical Mechanics in Electronic Packaging III (Houston, TX, 1-3 June 1998).
[8] J. Allen, M.A.M. Bourke, S. Dawes, M.T. Hutchings, and P.J. Withers, Acta Metall. Mater. **40**, 2361 (1992).
[9] D.C. Dunand, D. Mari, M.A.M. Bourke, and J.A. Roberts, Metall. Mater. Trans. **27A**, 2820 (1996).